



THE UNIVERSITY *of* EDINBURGH

Edinburgh Research Explorer

A preliminary investigation to develop a semi-probabilistic model of informal settlement fire spread using B-RISK

Citation for published version:

Cicione, A, Wade, C, Spearpoint, M, Gibson, L, Walls, R & Rush, D 2020, 'A preliminary investigation to develop a semi-probabilistic model of informal settlement fire spread using B-RISK', *Fire Safety Journal*. <https://doi.org/10.1016/j.firesaf.2020.103115>

Digital Object Identifier (DOI):

[10.1016/j.firesaf.2020.103115](https://doi.org/10.1016/j.firesaf.2020.103115)

Link:

[Link to publication record in Edinburgh Research Explorer](#)

Document Version:

Peer reviewed version

Published In:

Fire Safety Journal

General rights

Copyright for the publications made accessible via the Edinburgh Research Explorer is retained by the author(s) and / or other copyright owners and it is a condition of accessing these publications that users recognise and abide by the legal requirements associated with these rights.

Take down policy

The University of Edinburgh has made every reasonable effort to ensure that Edinburgh Research Explorer content complies with UK legislation. If you believe that the public display of this file breaches copyright please contact openaccess@ed.ac.uk providing details, and we will remove access to the work immediately and investigate your claim.



1 **A preliminary investigation to develop a semi-probabilistic model of informal settlement**
2 **fire spread using B-RISK**

3 Antonio Cicione ^{a,*}, Colleen Wade ^b, Michael Spearpoint ^c, Lesley Gibson ^d, Richard Walls ^a,
4 David Rush ^d

5 ^a Department of Civil Engineering, Stellenbosch University, Stellenbosch, South Africa

6 ^b Fire Research Group Limited, New Zealand

7 ^c OFR Consultants, Manchester, UK

8 ^d School of Engineering, University of Edinburgh, Edinburgh, UK

9 *Corresponding author email: acicione@sun.ac.za

10 **Abstract**

11 In South Africa alone, there are more than 5000 informal settlement fires a year, where a
12 single incident can leave up to 10000 people homeless. The government and local authorities
13 of countries with informal settlements, that extend over large areas, have no tools to simulate
14 fires to identify high risk areas, or to quantify the magnitude of an incident to which they may
15 need to respond. It is with this backdrop that the paper seeks to develop a semi-probabilistic
16 method to determine fire spread rates in informal settlements. Data from a full-scale fire
17 experiment is used to validate the fire spread rates predicted by B-RISK from which a
18 simplified semi-probabilistic analysis method is developed that can estimate fire spread rates
19 in informal settlements. B-RISK simulations are then compared to an actual informal
20 settlement fire incident to assess its predictive capabilities. The paper also discusses how the
21 effect of wind has been included and what additional features could be incorporated to obtain
22 more realistic informal settlement fire spread predictions. This work provides the first step in
23 a complex problem where it is difficult to accurately define input parameters.

24 **Keywords:** informal settlements, fire spread, ignition time, item-to-item ignition

25 **1. Introduction**

26 Informal settlements, also commonly known as shantytowns, slums or ghettos, are often
27 razed by large fires [1]. Informal settlements are extremely vulnerable to fire spread because
28 they are inherently characterized by poor infrastructure, lack of basic services, poorly
29 constructed structures and are generally overcrowded [2]. Informal Settlement Dwellings
30 (ISDs) are makeshift structures that are typically constructed from materials in the immediate
31 surroundings of the inhabitant [3]. Informal settlements and ISDs, along with how they
32 behave in fire, are extensively discussed in [3–6]. Although numerous fire spread
33 interventions have been proposed and implemented over the past decade [7], informal
34 settlement fires still cause the one billion vulnerable people that reside within these
35 settlements extreme losses (i.e. economic losses and death) on a daily basis [8]. Whilst fire
36 related fatalities have decreased in high income countries, they have increased in lower-to-
37 middle income countries. Additionally, it is expected that the population that reside in
38 informal settlements will increase to 1.2 billion in Africa alone by 2050 [2]. It is thus a cause
39 for serious concern to see how little work is done in terms of fire safety in these communities.

40 Aiming to better understand informal settlement fires and to assist local authorities in their
41 attempts to select the most suitable fire spread interventions, recent studies have investigated
42 the fire dynamics within ISDs and fire spread between ISDs [3,5,9–11]. Cicione and Walls
43 [9] looked at a simplified method to model ISD fire spread using Fire Dynamics Simulator

44 (FDS) simulations. They found that even with powerful software such as FDS, it is difficult
45 to predict fire spread rates between dwellings. Additionally, there are a significant number of
46 unknowns that are inherent in informal settlements. These include: during an incident, there
47 are suppression efforts by residents and firefighters; combustibles are present between, or on
48 top of dwellings; dwellings are poorly constructed so structural collapse occurs quickly after
49 ignition; dwellings have variable ventilation conditions; evacuating residents move their
50 possessions, resulting in mobile fuel loads that can be transferred into open ‘fuel break’ areas;
51 there are large variations in the construction products and the household content found; wind
52 can significantly influence fire spread rates; settlements are ever-changing meaning that
53 geometries are difficult to accurately quantify; gas canisters and liquid fuels may be stored in
54 the homes leading to small explosions; etc. Hence, in order to make any progress, it is
55 necessary to significantly simplify the problem. The work done in these previous studies
56 [3,5,9,10] are used as a basis for the semi-probabilistic analysis proposed in this work.

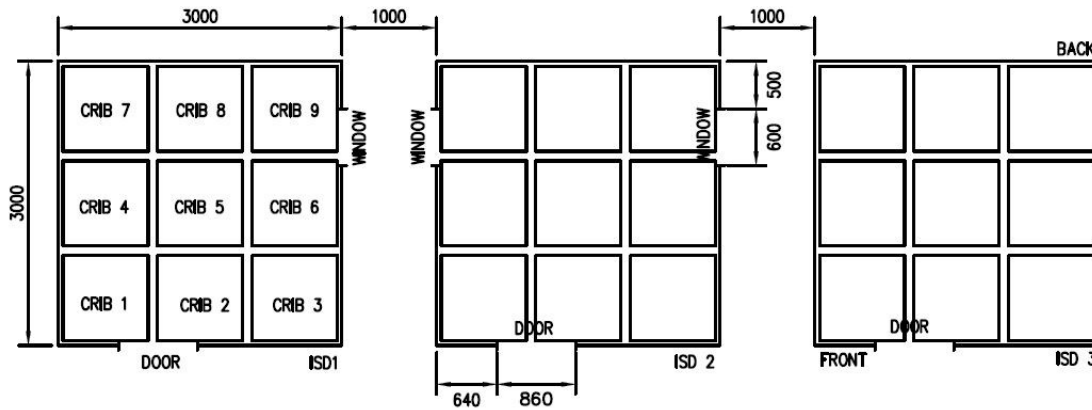
57 It is with this backdrop that this paper provides a preliminary method to estimate informal
58 settlement fire spread rates using B-RISK (version 2019.043), although other software, such
59 as Wildland-Urban Interface Fire Dynamics Simulator [12] could also have been used. The
60 hope is that the method developed can be generalized over time and refined so that it can aid
61 firefighters, municipal managers and community service organizations when dealing with
62 these unique fires. Ultimately, this work seeks to provide a semi-probabilistic model that
63 could assist authorities of countries with large informal settlements with a tool to simulate
64 fires to provide predictive capabilities that can help in identifying high risk areas, or quantify
65 the magnitude of an incident to which municipalities may need to respond. Single
66 deterministic answers regarding fire spread rates are not possible, and their usefulness is
67 questionable, but decision-making tools for quantifying fire risk would be invaluable. In
68 order to develop this semi-probabilistic model, the paper starts by developing an ISD spread
69 scenario (i.e. a baseline scenario), using B-RISK (a zonal model), for an ISD fire spread
70 experiment [3] with known fire spread rates. The experimental data is then used to validate
71 the initial B-RISK scenario input properties and are then used to create a semi-probabilistic
72 scenario in B-RISK. The software is then run for a real informal settlement fire and the
73 results are compared to the actual event to assess the performance of the software.

74 **2. Experiment used for baseline B-RISK scenario**

75 The baseline scenario that is assessed through B-RISK is based on an experiment consisting
76 of three steel clad ISDs. The experiment was conducted at the end of 2017 by the University
77 of Stellenbosch at the Breede Valley Fire Department, South Africa [3]. Fig.1 gives the
78 dimensions and details of the full-scale experiment, from which the geometries in the
79 baseline simulation have been created. The fuel load in each dwelling consisted of nine
80 timber (Pine) cribs, with 36 timber pieces (40×60×900 mm) per crib and was internally lined
81 with cardboard to mimic reality. The moisture content of the timber and cardboard was not
82 measured but can be assumed to be typical of normal ambient conditions. Fig. 1 was taken
83 from [9]. The wind speed on the day of the experiment was negligible according to [3], thus it
84 is ignored for the baseline scenario. For more details regarding this experiment the reader is
85 referred to [3].

86 The experimental fire spread rates are given in Table 1. The spread rates are taken as the time
87 between the start of flashover in each ISD, in which flashover was arbitrarily identified by a
88 ceiling temperature of 300 °C, i.e. approximately when the cardboard lining material ignites
89 [13,14] since this leads to the rapid onset of flashover, as discussed in [3,6].

90 For enclosures with non-combustible boundaries, flashover typically occurs when the upper
 91 layer reaches 500-600 °C, which corresponds to a radiative heat flux at the floor level of 15-
 92 20 kW/m² [15]. Thus, the initial fire growth time in the dwelling of origin is eliminated as
 93 this will vary from dwelling to dwelling, and event to event. Table 1 also gives a summary of
 94 the results obtained in [3]. The peak heat flux values in Table 1 were measured during the
 95 fully developed stage of the fire.



96
 97 Fig. 1. Overview of the experimental dimensions of (figure from [9], with permission from
 98 John Wiley and Sons)

99

100 Table 1: Summary of details from the steel triple ISD experiment [3,9]

	ISD 1	ISD 2	ISD 3
Spread mechanism	Dwelling of origin	Flame impingement on the cardboard	Flame impingement on the cardboard
Fire spread time [s]	N/A	210 (between the start of flashover in ISD1-ISD2)	182 (between the start of flashover in ISD2-ISD3)
Time from flashover to collapse [min]	8.5	6.3	8.4
Heat flux 1 m from the door [kW/m ²]	59	79	66

101

102 3. Radiation and target ignition in B-RISK

103 This section gives a brief introduction to the B-RISK radiation and ignition model used in
 104 this work. For a more in-depth explanation of B-RISK, the reader is referred to [16]. This
 105 section also describes a simple method implemented to account for the effect of wind.

106 3.1. Radiation

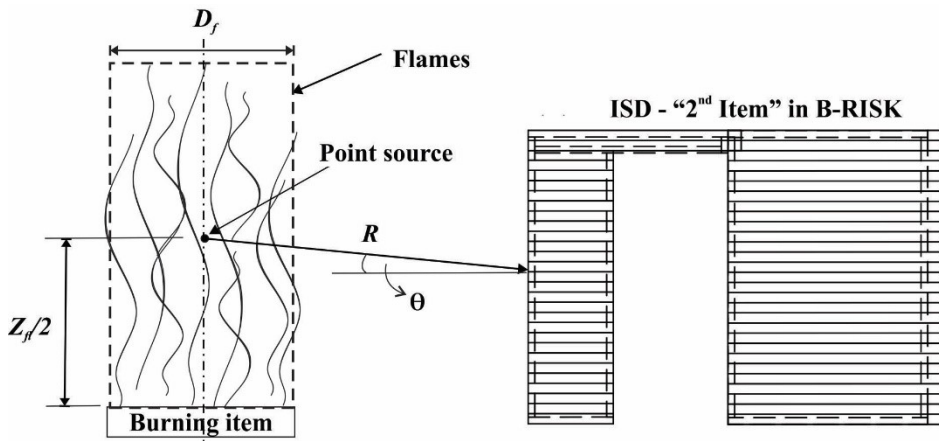
107 B-RISK models the ignition of secondary items through radiation from either the hot gas
 108 layer in an enclosure or from one or more already burning items. However, this work treats
 109 the objects as being outside and not within an enclosure so that no hot layer is present. To
 110 ensure a hot layer is not created in the simulations, the ‘enclosure’ is given a sufficient
 111 number of vents to allow the hot air to escape to the ‘outside’. Thus, the focus will be on an
 112 initial item igniting secondary items, i.e. the ISD of origin ‘item 1’ ignites the vertical

113 surfaces of adjacent ISDs ‘secondary or target items’ by means of radiation. Previous
 114 research [17] investigated the performance of different flame radiation models, namely: the
 115 spherical model (also known as the point source model, PSM), three different cylindrical
 116 models and a planar model. It was found that the PSM gave the best correlation with actual
 117 experimental heat flux results, and thus it is chosen for inclusion in the design fire generator
 118 (DFG) [18] submodel. The mathematical formula for the PSM is as follows:

$$119 \quad \dot{q}''_{fl} = \dot{Q}\chi_R \cos\theta / 4\pi R^2 \quad (1)$$

120 where \dot{q}''_{fl} is the heat flux received by the target item from the flaming item [kW/m²], \dot{Q} is the
 121 total heat release rate of the burning item [kW], χ_R is the radiative fraction and R is the
 122 horizontal radial distance from the center of the flaming region of the burning item (known as
 123 the point source) to the nearest point of the target item [m]. Fig. 2 shows the geometry
 124 assumed in this study where, in this case θ is zero, but it is shown for illustration purposes.
 125 The flame height z_{fl} [m] is calculated using Heskestad’s [19] correlation given by:

$$126 \quad z_{fl} = 0.235\dot{Q}^{2/5} - 1.02D_f. \quad (2)$$



127
 128 Fig. 2. PSM geometry between burning and target items, adapted from [20]

129 3.2. Effect of wind speed

130 Wind is a key factor affecting fire spread rates during informal settlements fire incidents [21].
 131 Since B-RISK mainly deals with enclosure fires, the need to adjust the radiation model for
 132 fire spread between objects to account for wind has been unnecessary to date. However, for
 133 the purpose of simulating fire spread in informal settlements, it is necessary to incorporate the
 134 effect of wind on flames in B-RISK. This work proposes a preliminary method to account for
 135 wind and is programmed into B-RISK for use in a later section to simulate a real informal
 136 settlement fire. It should be noted that since the main focus of this paper is to investigate a
 137 preliminary semi-probabilistic analysis to simulate fire spread in informal settlements, some
 138 simplifications have been made in terms of incorporating wind into B-RISK, i.e. that wind
 139 direction and the wind speed are constant throughout the simulation. However, in reality the
 140 wind direction and speed can change during a fire incident and, this should be incorporated in
 141 future versions of the method developed in this work.

142 Research by Thomas [22] and AGA [23] reported plume and flame shape properties of a
 143 single fire source in the presence of wind. More recently, Oka et. al [24] developed a formula
 144 (Eq. 3) to predict flame tilt angles for urban fires that is more applicable for practical use,
 145 where the empirical model developed for flame tilt angles is based on the balance of mass

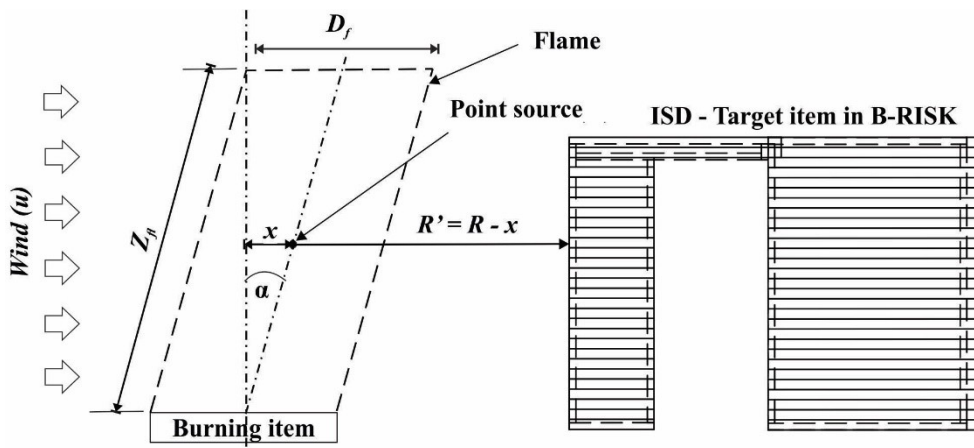
146 between the fluxes given by the upward hot current and the cross-wind. The formula is as
 147 follows:

$$148 \quad \tan \alpha = 2.73 Fr \frac{2}{5} \cdot Q^{*-0.1(1+2.5y)} \cdot \left(\frac{W}{r^*}\right)^{-0.5} \quad (3)$$

149 where α is the angle between the vertical line from the center of the burning item to the
 150 intersection of the wind-tilted flame axis, Fr is the Froude number given by u^2/gD (where u
 151 is the wind speed [m/s], D is the short length of the rectangular burning item [m] and g is the
 152 acceleration due to gravity [m/s²]), Q^* is the dimensionless heat release rate given by
 153 $\dot{Q}/(\rho_a C_p T_a g^{1/2} D^{5/2})$ (where \dot{Q} is the heat release rate [kW], ρ_a is the density of ambient air
 154 [kg/m³], C_p is the specific heat of constant pressure [kJ·kg⁻¹·K⁻¹] and T_a is the ambient
 155 temperature [K]), $y = 2$ for $0.05 < Q^* < 0.38$ and $y = 2/3$ for $0.38 < Q^* < 12.8$, W is the long length
 156 of the rectangular burning item, and $r^* = \sqrt{\text{burning item floor area}/\pi}$. Thus, in the presence
 157 of wind, the updated radial distance between the point source and the burning object (R') can
 158 be calculated as follows (see Fig. 3):

$$159 \quad R' = R - \frac{z_{fl}}{2} \cdot \sin \alpha \quad (4)$$

160 Refer to Fig. 3 below for a visual depiction of the variables used in Eq. 4. Since B-RISK only
 161 takes the radiation distance as the horizontal distance (in plan) between the two items, the
 162 point source height has not been modified.



163
 164 Fig. 3. PSM geometry between burning and target items when exposed to wind

165 3.3. Ignition

166 Following on from the work of Fleury [17] and the selection of the PSM within B-RISK,
 167 Baker *et al.* [25] published work examining the process of selecting an ignition criteria
 168 methodology for the submodel by establishing a set of essential criteria that the ignition
 169 method needs to meet. Baker *et al.* [25] determined that the flux-time product (FTP) method
 170 was sufficiently appropriate to simulate the ignition of secondary items, and it has been used
 171 in numerous other works [18,26–28]. The FTP method is a simplified approach to estimate
 172 ignition of combustible items subjected to an incident heat flux. The method was first derived
 173 by Smith and Satjia [29], which other researchers later extended. The method was then
 174 generalized by Shields *et al.* [30] such that:

$$175 \quad FTP = t_{ig}(\dot{q}'' - \dot{q}_{cr}'')^n \quad (5)$$

176 where t_{ig} is the time-to-ignition, \dot{q}'' is the incident heat flux emitted by the burning item (i.e.
177 \dot{q}''_{fl} calculated using Eq. 1), \dot{q}''_{cr} is the critical heat flux [kW/m²] and n is known as the FTP
178 index and can be obtained by plotting $1/t_{ig}^{1/n}$ against \dot{q}'' , and iteratively vary n to get the
179 best linear trend line fit [26]. The FTP index depends on the thermal thickness of the material.
180 As a guideline, a material is assumed to be thermally thin if $n = 1$, when $n = 1.5$ the material
181 is thermally intermediate, and when $n = 2$ the material is thermally thick [26].

182 The FTP method was originally limited to piloted ignition, however Baker *et al.* [25]
183 extended the method by deriving an empirical approximation for spontaneous ignition based
184 on the presence of a hot layer within an enclosure. It is therefore not applicable to the present
185 study as a hot layer is not permitted to be established in the model. Thus, in this work, the
186 focus will be on dwelling ignition by means of piloted ignition of vertical surfaces (i.e. as a
187 result of flame impingement from dwelling to dwelling for closely spaced ISDs in reality).
188 The FTP index is derived from cone calorimeter data of the cardboard lining used in the
189 experiments described above, since cardboard is typically used for lining material in informal
190 settlements [3]. The cardboard of an adjacent dwelling is typically exposed to the radiation
191 emitted by the burning dwelling as a result of poor construction methods, or gaps as a result
192 of the flutes of the corrugated sheets [6]. It should be noted that this is a conservative
193 assumption and that some dwellings are lined with other materials (e.g. timber) that have a
194 higher critical heat flux.

195 Currently there is negligible data on firebrand generation during large informal settlement
196 fires, although it is likely to occur. Discussions with firefighters and observations during
197 large-scale experiments (which may lack the materials required to create brands) have
198 provided insufficient data. Hence, firebrand behavior has been neglected in the current work,
199 and research is required to understand this phenomenon.

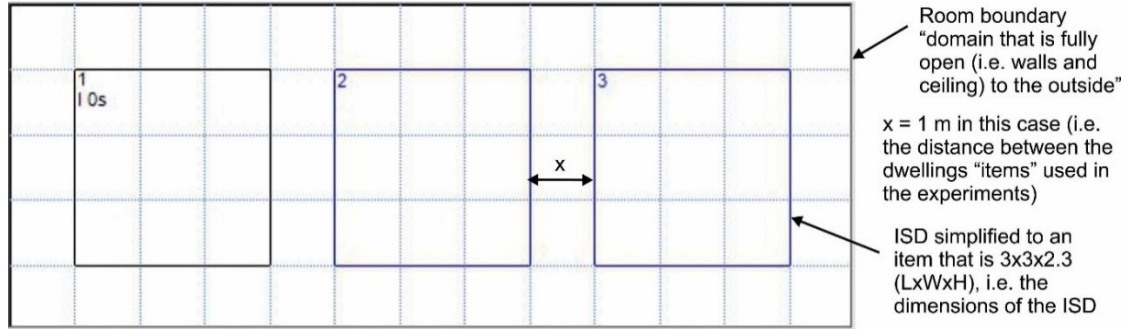
200 **4. B-RISK baseline scenario**

201 Before the inputs of the baseline scenario are discussed, it is important to note how the ISDs
202 experiment has been modelled and what simplifications are made. In order to simulate the
203 ignition of secondary dwellings in B-RISK, they must be simplified to items with a specific
204 shape (i.e. the volume of the ISD in this case) and a specific heat release rate (i.e. the heat
205 release rate of the ISD in this case).

206 The purpose of this scenario is to validate the ignition (FTP) input parameters by comparing
207 the B-RISK simulation results to the experimental results discussed above. The inputs are
208 then used to run a semi-probabilistic analysis (using Monte Carlo with stratified sampling,
209 where the ISDs were stratified based on dwelling floor area) on the Imizamo Yethu informal
210 settlement fire [21], by randomly populating ISDs (the 'items' in B-RISK) in an informal
211 settlement and simulating the scenario for a number of iterations. It should be noted that the
212 ignition predictions in B-RISK are not influenced by the material properties, combustion
213 properties of the item or the enclosure boundaries, other than the properties used in Eq. 1 and
214 Eq. 5 [26]. Thus, the ignition predictions are only dependent on the radiation from the flame
215 of the burning item(s) using the PSM and FTP formulae given by Eq. 1 and Eq. 5,
216 respectively. Where multiple items are burning, the incident heat (Eq. 5) on an adjacent item
217 (not yet ignited item) is the sum of that received from all the burning items, irrespective of
218 orientation, which is a conservative assumption.

219 **4.1. Input specification**

220 Fig. 4 depicts the geometric setup of the B-RISK baseline simulation, with the descriptions
 221 referring to what is discussed above. In this case the room ('domain') used is 13×5×6 m
 222 (L×W×H) and the three ISD items are given a size of 3×3×2.3 m (L×W×H), i.e. the actual
 223 size of the dwellings with each having a floor area of 9 m². As mentioned above, the wind
 224 speed was negligible during the experiment and it is thus not considered for the baseline
 225 simulation.



226

227 Fig. 4. Room setup in B-RISK (where ISD1-3 are modelled as items)

228 The next step is to define the combustion and ignition properties of the ISD items. The
 229 combustion properties are taken as those of the timber cribs used in [3], whereas the ignition
 230 properties are based on the cardboard lining used in [3]. The soot yield of 0.015 g/g, CO₂ of
 231 1.33 g/g and radiant loss fraction χ_R of 0.3 are taken from Table 3-4.14 of the SFPE
 232 Handbook [31]. The heat of gasification (1.8 kJ/g) has been selected from Table 3-4.7 of the
 233 SFPE Handbook [31], based on similar representative materials. Assuming a combustion
 234 efficiency of 1, the effective heat of combustion equals the gross heat of combustion heat of
 235 combustion (18 kJ/g) of the timber used in [3].

236 Unfortunately, the heat release rates (HRRs) were not measured during the experiment. Thus,
 237 similar to [6,9], the HRRs are calculated by the following formula [32]:

238
$$\dot{Q} = \dot{m}\Delta H_{\text{eff}} \quad (6)$$

239 where \dot{m} is the mass loss rate measured in kg/s (of the timber cribs in this case) and ΔH_{eff} is
 240 the effective heat of combustion (kJ/kg). The maximum HRR of the ISDs is taken as the
 241 maximum HRR of the timber cribs used as the fuel, based on the assumption that the
 242 cardboard lining contributes only a minor amount. The mass loss rate of the timber cribs, \dot{m} ,
 243 would normally be taken as the lesser of the surface-controlled mass loss rate, porosity-
 244 controlled mass loss rate, and the ventilation-controlled mass loss rate. However, here it is
 245 assumed that the mass loss rate is governed by ventilation [3,6,33–35], such that for the steel
 246 clad dwellings the mass loss rate is given by [32]:

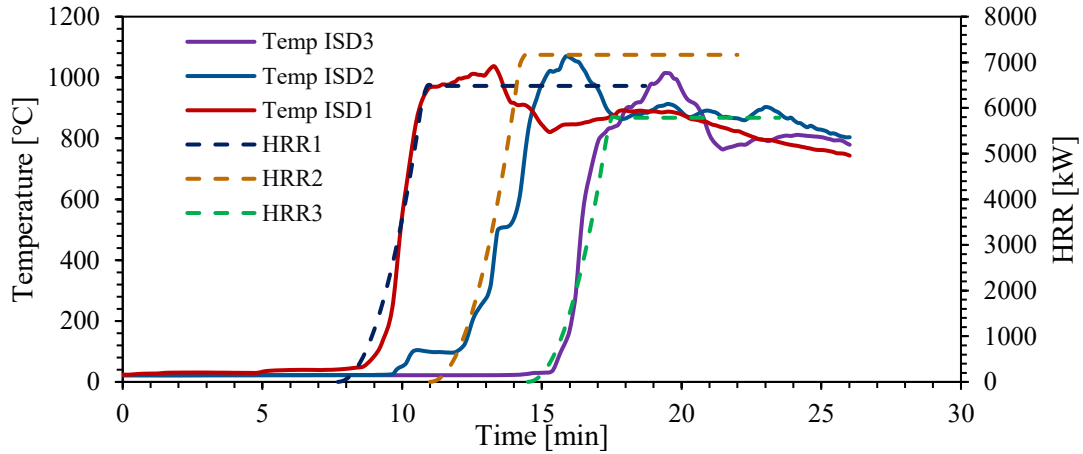
247
$$\dot{m} = 0.12A_v\sqrt{H_v} \quad (7)$$

248 where A_v is the sum of the areas of the openings in which $A_v = 2.29 \text{ m}^2$, $A_v = 2.65 \text{ m}^2$ and A_v
 249 $= 1.93 \text{ m}^2$ for ISD1, 2 and 3, respectively (A_v includes the openings created by the flutes). H_v
 250 is the weighted average of the heights of the openings and in this case $H_v = 1.72 \text{ m}$, $H_v =$
 251 1.57 m and $H_v = 1.93 \text{ m}$ for ISD1, 2 and 3, respectively. The weighted average is given by:

252
$$H_v = (H_1A_1 + H_2A_2 \dots)/A_t \quad (8)$$

253 where H_1 and A_1 is the height and area of the first opening, H_2 and A_2 is the height and area of
 254 the second opening and A_i is the sum of all the openings.

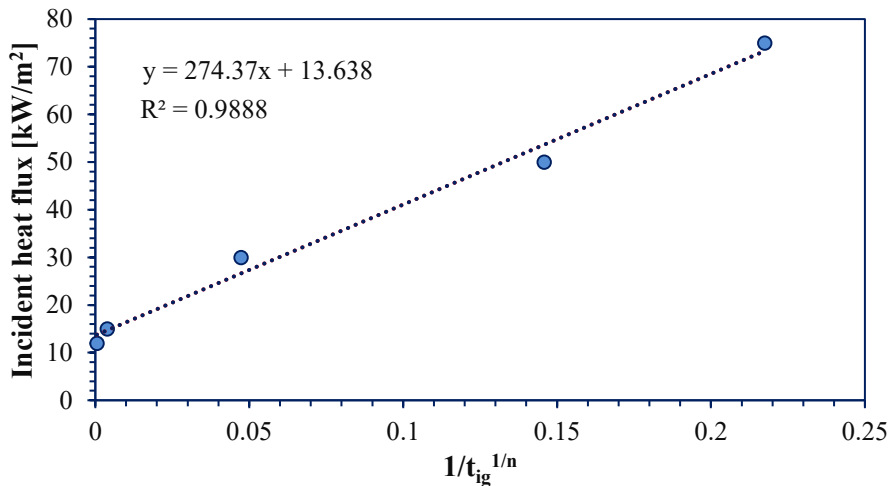
255 The growth phase is assumed to correspond with the experiment [6] (i.e. as seen by the time-
 256 temperature curves), which were very similar to a t-squared fire with an ultra-fast growth
 257 constant (k), thus a t-squared fire with $k = 75$ has been used in the baseline simulation. Fig. 5
 258 depicts the time-temperature curves of ISD1-3 of the steel-clad dwelling experiment along
 259 with the calculated HRR curves. For the steel clad dwellings, structural collapse was assumed
 260 to be 7.1 minutes (i.e. the average of the values listed in Table 1) after the fully developed
 261 fire stage was reached [34].



262

263 Fig. 5. HRR and ceiling temperatures versus time for ISD1-3

264 The last step is to define the ignition mechanism of the ISDs' items, and it is assumed to be
 265 the ignition of the cardboard lining. As mentioned earlier, by plotting \dot{q}'' against $1/t_{ig}^{1/n}$,
 266 both the value for n and FTP can be obtained by iteratively varying n to obtain the trendline
 267 with the highest correlation coefficient (R^2). Piloted ignition measurements from the cone
 268 calorimeter for the cardboard used in the large-scale experiments can be seen in Fig. 6.



269

270 Fig. 6. Correlation of ignition times and incident heat flux (cone calorimeter data from [14])

271 Wang *et al.* [14] found that the critical heat flux (CHF) of cardboard is somewhere between
 272 11 kW/m² and 12 kW/m², thus it is assumed that the CHF is 11.5 kW/m². The value of n is
 273 found to be equal to 1.39 with $R^2 = 0.9888$ and FTP is found to be equal to 2446 [kW/m²]ⁿ.

274 Using the above mentioned as direct inputs to the B-RISK baseline scenario yield the results
 275 discussed in the next section.

276 **4.2. Results and discussion**

277 Table 2 summarizes the experimental and B-RISK simulation spread rates of the dwellings.
 278 The percentages reported in brackets, indicate by what percentage the simulation overpredict
 279 (+) or underpredict (-) the spread rate. For the simulations, the spread rates are taken as the
 280 time between ignition of ISD item 1 to the ignition of the particular item under consideration,
 281 whereas the spread rates of the experiment are taken as the time between the start of flashover
 282 in ISD1 to the start of flashover in the particular dwelling under consideration. From Table 2
 283 it is clear that the B-RISK simulation with no wind slightly underpredicts the experimental
 284 data in terms of ignition times. The effect of wind is also assessed using the baseline scenario,
 285 with the wind direction being from left to right of the setup as depicted in Fig. 4. It is clear
 286 that as the wind speed increases the spread rate increases, indicating that the wind
 287 functionality added to B-RISK works as expected. For higher wind speeds, the spread rates
 288 start to converge, simply indicating that for these particular dwelling sizes and HRRs, the tilt
 289 angle is starting to approach the maximum tilt angle, at a wind speed of approximately
 290 10 m/s. In order to get the best correlation to the experimental results, the simulation has been
 291 calibrated by decreasing the value of n . It is found that $n = 1.57$ gives the best correlation to
 292 the experimental results, thus it is decided to use $n = 1.57$ for the case study simulations that
 293 follow.

294 Table 2: Summary of baseline simulation results versus experimental results

Experiment/Model	Time to ignition after the ignition of ISD1 [s]	
	ISD2	ISD3
Experiment (Negligible wind)	210	392
B-RISK simulation (No wind)	231 (-10%)	433 (+10.46%)
B-RISK simulation (1 m/s wind)	145 (+30.95%)	283 (+27.8%)
B-RISK simulation (5 m/s wind)	138 (+34.29%)	269 (+31.4%)
B-RISK simulation (10 m/s wind)	138 (+34.29%)	269 (+31.4%)
B-RISK (No wind, $n = 1$)	178 (+15.2%)	338 (+13.8%)
B-RISK (No wind, $n = 1.57$)	208 (+0.95%)	395 (-0.77%)

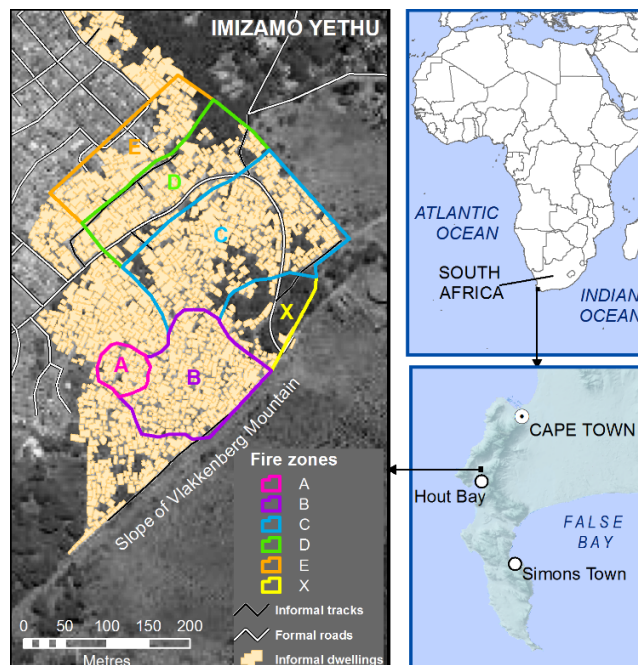
295 **5. Semi-probabilistic simulation of the 2017 Imizamo Yethu fire**

296 The purpose of this section is to use the input data used in the baseline scenario, but with $n =$
 297 1.57 and apply it to a real informal settlement. The results are then compared to a fire
 298 incident that occurred in the settlement of interest. It should be noted that the slope of the
 299 settlement is not accounted for as the current version of B-RISK does not have the
 300 functionality to account for this. Additionally, B-RISK currently cannot account for
 301 fluctuations in wind speed or fluctuations in wind directions, as mentioned earlier. In terms of
 302 the Imizamo Yethu fire, the wind speed fluctuated between 7.8 m/s (28 km/h) - 12.8 m/s
 303 (46 km/h), and the wind direction changed by a full 180 degrees during the incident. Thus,
 304 these factors may be incorporated in future versions of B-RISK, as more case studies become
 305 available for calibration.

306 **5.1. Imizamo Yethu 2017 fire**

307 Imizamo Yethu is an informal settlement in the Hout Bay Valley, on the Atlantic Ocean side
308 (west) of the Cape Peninsula, and within the jurisdiction of the City of Cape Town. The
309 settlement is situated on steep (average 12° slope) mountain land with poor access thus
310 limiting the ability of emergency services to reach the upper parts of the settlement as the
311 road access deteriorates with steepness of slope [36]. Imizamo Yethu is notorious for its lack
312 of basic services and infrastructure. The exact number of occupants is unknown but is
313 estimated in the region of 16000 to 36000 [37] with a settlement density ranging from 228 –
314 262 dwellings per hectare. Imizamo Yethu has a long history of fire [38] and, prior to the
315 2017 fire discussed in this paper, a fire in 2004 destroyed 1200 informal dwellings and left as
316 many as 5000 residents homeless.

317 As described in detail by Kahanji *et al.* [21], on the night of Saturday 11 March 2017, at
318 around 00h00, a fire started in Imizamo Yethu and was finally extinguished thirteen hours
319 later at around 13h00 on Sunday 12 March 2017. This devastating fire resulted in four deaths,
320 two fire fighter injuries, 2194 structures destroyed and approximately 9700 people displaced
321 [21]. Kahanji *et al.* [21] divided the burn scar into zones on the basis of fire fighters’ reports
322 of the location and time of the fire front. The fire started in Zone A (Fig. 7) and it appears that
323 the inhabitants in the dwelling of origin perished in the blaze. Fire fighters arrived on the
324 scene and the fire appeared to be almost under control, but a resident cut the fire fighters hose
325 to direct water to their own home and from this point on, the fire quickly grew, pushed by
326 wind and topography. The wind changed direction between 01h00 and 03h00 from Northeast
327 to Southwest which then pushed the fire beyond Zone A and into Zones B and C. In this
328 work, the semi-probabilistic model will be focused on fire spread modelling within Zone A
329 (average 9° slope), thus the rest of the fire report is not summarized here, however a
330 description of the fire in Zones B – E can be accessed in Kahanji *et al* [21].



331
332 Fig. 7. The Location of Imizamo Yethu and the fire of 11 March 2017, showing the fires
333 zones as determined by Kahanji *et al.* [21].

334 **5.2. Zone A**

335 The fire zones delineated by Kahanji *et al.* [21] were determined roughly from the fire
 336 fighters' reports at settlement scale without individual dwellings being considered. It can be
 337 seen in Fig. 8 that this delimitation results in some dwellings being considered partly in and
 338 partly out of the fire extent and dwellings straddle the boundary between zones. When
 339 considering the detail require for modelling fire spread, Zone A's boundaries have been
 340 redefine, and the boundary has been adjusted along dwelling boundaries so that dwellings are
 341 either completely included or completely excluded from Zone A. Thus, the revised area of
 342 Zone A (Fig. 9) is 3312 m². Dwellings were digitized in ArcGIS 10.5 at a scale of 1:200 from
 343 City of Cape Town high resolution (~8 cm resolution) aerial photography captured on
 344 February 2017, approximately one month before the fire. Some dwellings are built very close
 345 or even touching each other, making delimiting individual dwellings challenging. Generally,
 346 where a gap, however small, between dwellings could be detected, dwellings were digitized
 347 as individual dwellings. Further, very large continuous structures were delimited into
 348 multiple dwellings based on shape of the structure and identification of differing roof
 349 sheeting. A large tree in Zone A partially obscured roofs of dwellings and the outline of these
 350 dwellings was estimated by extending the roof boundaries where visible. Area statistics for
 351 all dwellings in Zone A were calculated and the frequency distribution of the size of
 352 dwellings were plotted, as depicted in Fig. 10.



Fig. 8. Original fire Zone A

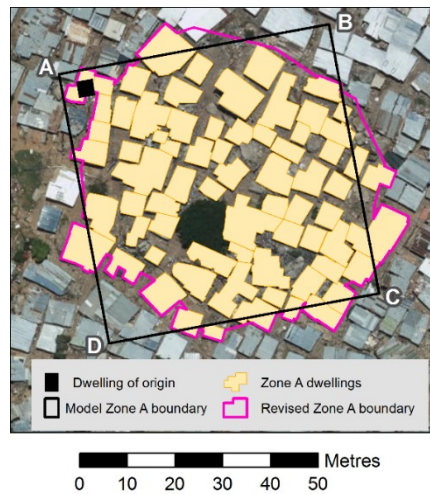
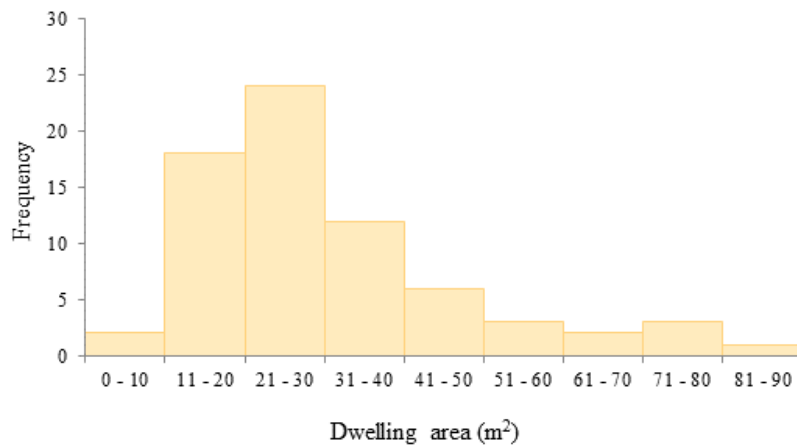


Fig. 9. Revised fire Zone A



353
 354 Fig. 10. Frequency distribution of the size of dwellings in Imizamo Yethu Zone A

355 From these statistics, together with the calculated area of Zone A, the following metrics can
 356 be obtained: (a) the dwelling density: Total dwelling area represented as a percentage of Zone
 357 A area is 65.28%, (b) the household density: Number of individual dwellings within Zone A,
 358 upscaled to number of dwellings per hectare is 214 dwellings/ha, a figure close to the
 359 reported settlement density of 228 – 262 dwellings/ha, and (c) the dwelling roof area (which
 360 is assumed to be equal to the floor area) ranges from $\sim 7 \text{ m}^2$ to 86 m^2 (although it is possible
 361 that the large dwellings represent more than one household) with the frequency distribution
 362 peaking at around 22 m^2 .

363 5.3. Semi-probabilistic model setup

364 To represent Zone A, an area of $58 \text{ m} \times 58 \text{ m}$ (see Fig. 9) populated with 71 ISD items Fig.
 365 10) at locations randomly allocated by B-RISK, as depicted in Fig. 12, within the Zone is
 366 simulated. The ISD item size distributions are taken from Fig. 10. Thus, only the locations of
 367 the 71 items are varied from simulation to simulation, with all other inputs remaining
 368 constant. Assigning probabilistic distributions to variables such as n , FTP, HRRPUA etc., to
 369 account for more of the variables in informal settlements would be beneficial. It should
 370 however be noted that the current version of B-RISK does not have the functionality to assign
 371 a probabilistic distribution for all of these variables and should thus be coded into B-RISK.
 372 Since this is only the first attempt and since space is limited, it is recommended for future
 373 work. Since the opening sizes and the number of openings per dwelling for the case study
 374 scenario are not known, some assumptions are needed. Thus, it is assumed that the dwellings
 375 are always ventilation controlled, such that the HRR curve assigned to the dwellings are the
 376 HRR curves as depicted in Fig.5 multiplied by a factor f_A which is the ratio of the area of the
 377 dwelling under consideration to the area of the dwelling representing the original HRR (the
 378 original item being one of the dwellings used in the triple steel clad experiment). Thus, it is
 379 assumed that H_v (Eq. 7) remains approximately constant, but that A_v (Eq. 7) increases
 380 proportional to the dwelling floor area. Table 3 lists the number of dwellings with their
 381 associated dwelling size, HRR curve (decided in such a way that each curve is used roughly
 382 the same number of times) and f_A .

383 Table 3: Model inputs summarizing assumptions for dwelling characteristics

Dwelling size (L×W×H)	Number of dwellings	Original HRR curve used	f_A
3.5 m × 3.5 m × 2.3 m	1	ISD1	1.4
3 m × 3 m × 2.3m	5	ISD1	1.0
3.5 m × 3.5 m × 2.3m	9	ISD1	1.4
4 m × 4 m × 2.3m	13	ISD2	1.8
4.5 m × 4.5 m × 2.3m	15	ISD3	2.3
5 m × 5 m × 2.3m	11	ISD1	2.8
5.5 m × 5.5 m × 2.3m	2	ISD2	3.4
6 m × 6 m × 2.3m	3	ISD2	4.0
6.5 m × 6.5 m × 2.3m	5	ISD2	4.7
7 m × 7 m × 2.3m	2	ISD3	5.4
8 m × 8 m × 2.3m	4	ISD3	7.1
9 m × 9 m × 2.3m	1	ISD3	9.0

384

385 **5.4. Results and discussion**

386 Two scenario variations (i.e. one with wind and one without wind) have been executed with
 387 the resulted averages displayed in Fig. 11. Currently B-RISK does not generate an output file
 388 for the spread time between dwellings. Thus, since the spread rates were captured by hand,
 389 only 100 simulations were run to illustrate the functionality of the model. Note that the
 390 location of the first item ignited was always fixed to the bottom left of the domain. The fire
 391 spread rates here are different than above and is given in m^2/hr . This has been calculated by
 392 dividing the total domain area by the time it took to ignite all the items (similar to what was
 393 done in [21]). The wind speed of 8.9 m/s used, is based on the actual wind speed during the
 394 fire incident of 8.9 m/s (32 km/h) as reported in [21] with a wind direction of 45 degrees, as
 395 depicted in Fig. 12. The error bar for Zone A is based on the start time of the incident. In this
 396 case, it is assumed that the fire started at 00:00 (although it could have started slightly earlier
 397 or later). The spread rate for Zone C and D are also added to Fig. 11 to show the range of
 398 spread rates that occurred during the incident. The error bars of the B-RISK results are the
 399 standard deviation of the simulations. The black dwelling in the bottom left corner of Fig. 12
 400 represents the dwelling of origin (the position was fixed for all simulations).

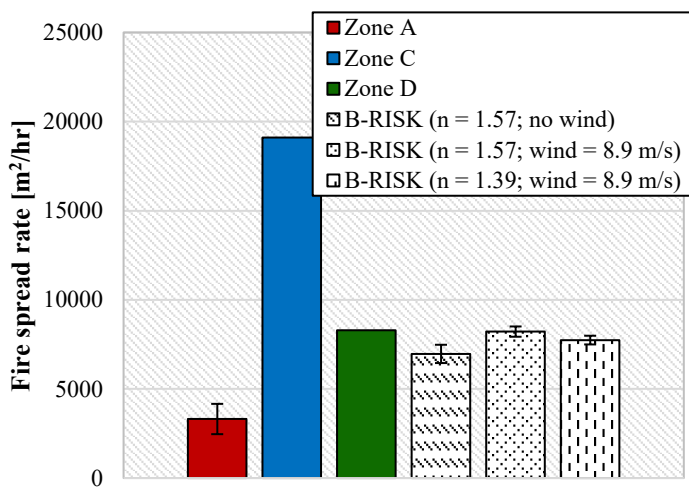


Fig. 11. Fire spread rates of Zone A, C and D and the B-RISK simulation

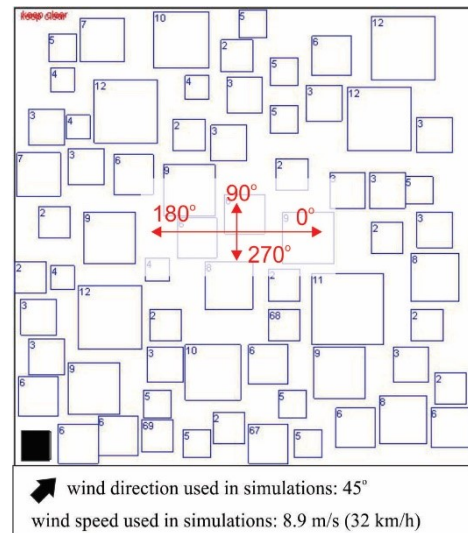


Fig. 12. Wind direction angles and an example of random item population

401 Based on the B-RISK simulations, a wind speed of 8.9 m/s increases the spread rate by
 402 $1252 m^2/hr$ on average, consistent with the baseline scenario and showing that wind
 403 functionality added to B-RISK works as expected. The actual fire spread rate in Zone A of
 404 $3312 m^2/hr$ is slower than the predicted B-RISK spread rate (wind included) of $8216 m^2/hr$.
 405 This could be due to multiple reasons, such as: B-RISK not accounting for human
 406 intervention (i.e. fire brigade and inhabitants); Zone A boundaries being approximate
 407 boundaries based on fire fighters' interviews; not only cardboard is used for lining materials
 408 in reality (with more data this can be calibrated). The B-RISK error bars shown are relatively
 409 narrow – there are still many uncertainties not included in the analysis such as the materials
 410 and their ignition and combustion properties, uncertainty in the flame shape and size, view
 411 factors etc. The only uncertainty included in the analysis is the randomization of the ISD
 412 locations, and there are additional uncertainties associated with the assumed ISD density. The
 413 predicted spread rate of $8216 m^2/hr$ is however plausible when compared to the $8300 m^2/hr$

414 spread rate of Zone D. Zone C had a spread rate of 19100 m²/hr, indicating that much higher
415 spread rates are also possible. The higher spread rate, in Zone C, can be as a result of many
416 reasons such as an increase in wind speed, as the fire gets bigger it results in more rapid
417 spread and human intervention has less of an effect as the fire grows. Considering all the
418 variables and unknowns, the predicted spread rate of 8216 m²/hr is a good first step in the
419 development of this semi-probabilistic method to simulate fire spread in informal settlements.
420 Interestingly, a simulation executed with $n = 1.39$ (the original n value for the cardboard),
421 shows a fire spread rate of 7740 m²/hr which is closer to the actual incident, compared to the
422 spread rate of 8216 m²/hr obtained with $n = 1.57$.

423 6. Future considerations

424 This paper develops a preliminary semi-probabilistic model of informal settlement fire spread
425 using B-RISK, through making a number of assumptions. As more data becomes available
426 from informal settlement dwelling experiments and from real fire incidents, the model
427 discussed can be calibrated and updated to account for more variables, and to make it more
428 practical for municipalities and fire brigades to use as a tool for risk and strategy planning.
429 For future work it is recommended that variables such as FTP, n , HRR, etc. are randomly
430 generated from a probabilistic distribution, in order to account for more of the unknowns
431 associated with informal settlements. Additionally, the following needs to be
432 implemented/considered in future versions: (a) the ability to vary wind speeds and directions,
433 (b) graphical outputs of the fire spread patterns, (c) the ability to auto-populate different
434 ignition criteria (i.e. to account for a number of possible lining/cladding materials), (d) the
435 ability to slope the floor of the 'domain', (f) the ability to specify variations in the 'room' and
436 'item' shapes, and (e) the ability to include vegetation or random combustibles between
437 dwellings as one would typically find in informal settlements.

438 7. Conclusions

439 This work provides the first step towards the development of tools to simulate fire spread in
440 informal settlements, in order to provide municipalities with predictive capabilities in
441 identifying high risk areas, or to quantify the magnitude of an incident to which
442 municipalities may need to respond to. This first step includes the development of a
443 methodology using B-RISK, determining ignition criteria that best fit ISDs, implementing a
444 simplified method to account for wind, and the execution of a validation and case study
445 scenario. The baseline scenario, with a total spread time of 392 s, shows a good correlation
446 compared to the experimental results, with a total spread time of 374 s. The baseline scenario
447 inputs are thus used to model the case study scenario, where it is found that the B-RISK
448 simulation over-estimates the fire spread rate in Zone A by 5004 m²/hr. However, since the
449 simulation neglect factors such as human intervention, it was expected that the simulation
450 would over-predict the spread rate. The predicted spread rate seems plausible when compared
451 to other zones (Zone C and D). Considering the complexity of the problem and the difficulty
452 to accurately define input parameters, this paper is a first step to simulate fire spread in
453 informal settlements. With more than one billion people residing in informal settlements
454 there is a need to understand and improve fire safety in these areas.

455 8. Acknowledgements

456 Aerial photography was obtained from the City of Cape Town via the Open Data portal. The
457 authors would like to acknowledge the financial support of the Global Challenges Research

458 Fund (GCRF of the EPSRC) under unique grant number EP/P029582/1, and the Lloyd's
459 Register Foundation under the "Fire Engineering Education for Africa" grant.

460 9. References

- 461 [1] UN Office for Disaster Reduction, UNISDR Terminology on Disaster Risk Reduction,
462 Geneva, Switzerland, 2009. <https://doi.org/978-600-6937-11-3>.
- 463 [2] UN-Habitat, Slum Almanac 2015/2016: Tackling Improvement in the Lives of Slum
464 Dwellers, Nairobi, 2016.
- 465 [3] A. Cicione, R.S. Walls, C. Kahanji, Experimental study of fire spread between
466 multiple full scale informal settlement dwellings, *Fire Saf. J.* 105 (2019) 19–27.
467 <https://doi.org/10.1016/j.firesaf.2019.02.001>.
- 468 [4] P. Zweig, R. Pharoah, R. Eksteen, R.S. Walls, Installation of Smoke Alarms in an
469 Informal Settlement Community in Cape Town, South Africa – Final Report, 2018.
- 470 [5] R.S. Walls, C. Kahanji, A. Cicione, M. Jansen van Vuuren, Fire dynamics in informal
471 settlement "shacks": Lessons learnt and appraisal of fire behavior based on full-scale
472 testing, in: 11th Asia-Oceania Symp. Fire Sci. Technol., Taiwan, 2018.
- 473 [6] A. Cicione, M. Beshir, R.S. Walls, D. Rush, Full-Scale Informal Settlement Dwelling
474 Fire Experiments and Development of Numerical Models, Springer US, 2019.
475 <https://doi.org/10.1007/s10694-019-00894-w>.
- 476 [7] R.S. Walls, R. Eksteen, C. Kahanji, A. Cicione, Appraisal of fire safety interventions
477 and strategies for informal settlements in South Africa, *Disaster Prev. Manag.* 28
478 (2019) 343–358. <https://doi.org/https://doi.org/10.1108/DPM-10-2018-0350>.
- 479 [8] FPASA, SA Fire Loss Statistics 2015, 2017.
- 480 [9] A. Cicione, R.S. Walls, Towards a simplified fire dynamic simulator model to analyse
481 fire spread between multiple informal settlement dwellings based on full-scale
482 experiments, *Fire Mater.* (2020) 1–17. <https://doi.org/10.1002/fam.2814>.
- 483 [10] R. Walls, P. Zweig, Towards sustainable slums : understanding fire engineering in
484 informal settlements, *Sustain. Vital Technol. Eng. Informatics.* (2016) 1–5.
- 485 [11] M. Beshir, Y. Wang, L. Gibson, S. Welch, D. Rush, A Computational Study on the
486 Effect of Horizontal Openings on Fire Dynamics within Informal Dwellings, *Proc.*
487 *Ninth Int. Semin. Fire Explos. Hazards (ISFEH9).* (2019) 512–523.
488 <https://doi.org/10.18720/spbpu/2/k19-122>.
- 489 [12] W. Mell, A. Bova, G. Forney, Models for Fire Spread in the Wildland-Urban Interface,
490 (2012) 1–61.
- 491 [13] E. Kim, N. Dembsey, Engineering Guide for Estimating Material Pyrolysis Properties
492 for Fire Modeling, 2012.
- 493 [14] Y. Wang, C. Bertrand, M. Beshir, C. Kahanji, R. Walls, D. Rush, Developing an
494 experimental database of burning characteristics of combustible informal settlement
495 dwelling materials, *Fire Saf. J.* (2019).
496 <https://doi.org/https://doi.org/10.1016/j.firesaf.2019.102938>.
- 497 [15] D. Drysdale, An Introduction to Fire Dynamics, 3rd ed., John Wiley & Sons, LTD,
498 2011.

- 499 [16] C. Wade, G. Baker, K. Frank, R. Harrison, M. Spearpoint, B-RISK user guide and
500 technical manual, BRANZ Study Report SR364, Porirua, New Zealand, 2013.
- 501 [17] R. Fleury, M. Spearpoint, C. Fleischmann, Evaluation of Thermal Radiation Models
502 for Fire Spread Between Objects, in: Fire Evacuation Model. Tech. Conf., Baltimore,
503 Maryland, 2011. <http://www.ir.canterbury.ac.nz/handle/10092/4959>.
- 504 [18] G. Baker, P.C. Collier, C. Wade, M. Spearpoint, C.M. Fleischmann, K. Frank, S.
505 Sazegara, A comparison of a priori modelling predictions with experimental results to
506 validate a design generator submodel, in: 13th Int. Fire Mater. Conf., San Francisco,
507 CA, USA, 2013.
- 508 [19] G. Heskestad, Fire Plumes, Flame Height, and Air Entrainment, in: SFPE Handb. Fire
509 Prot. Eng., 4th ed., Quincy, MA, USA, 2008: pp. 2–1 to 2–20.
- 510 [20] G. Baker, M. Spearpoint, C. Fleischmann, C. Wade, Development of a Radiative Fire
511 Spread Submodel for an Enhanced Zone Model, in: 8th Asia-Oceania Symp. Fire Sci.
512 Technol., International Association of Fire Safety Science, 2010.
- 513 [21] C. Kahanji, R.S. Walls, A. Cicione, Fire spread analysis for the 2017 Imizamo Yethu
514 informal settlement conflagration in South Africa, *Int. J. Disaster Risk Reduct.* (2019).
515 <https://doi.org/10.1016/j.ijdr.2019.101146>.
- 516 [22] P.H. Thomas, The Size of Flames from Natural Fires, in: 9th Int. Combust. Symp.,
517 Combustion Institute, 1963: pp. 844–859.
- 518 [23] American Gas Association, Report IS 3-1, 1974.
- 519 [24] Y. Oka, O. Sugawa, T. Imamura, Y. Matsubara, Effect Of Cross-Winds To Apparent
520 Flame Height And Tilt Angle From Several Kinds Of Fire Source, in: *Fire Saf. Sci.*,
521 2003: pp. 7:915-926. <https://doi.org/10.3801/IAFSS.FSS.7-915>.
- 522 [25] G. Baker, M. Spearpoint, C. Fleischmann, C. Wade, Selecting an ignition criterion
523 methodology for use in a radiative fire spread submodel, *Fire Mater.* 35 (2011) 367–
524 381. <https://doi.org/10.1002/fam.1059>.
- 525 [26] S. Sazegara, M. Spearpoint, G. Baker, Benchmarking the Single Item Ignition
526 Prediction Capability of B-RISK Using Furniture Calorimeter and Room-Size
527 Experiments, *Fire Technol.* 53 (2017) 1485–1508. <https://doi.org/10.1007/s10694-016-0642-y>.
- 529 [27] G. Baker, R. Fleury, M. Spearpoint, C.M. Fleischmann, C. Wade, Ignition of
530 Secondary Objects in a Design Fire Simulation Tool, in: *Fire Saf. Sci.*, 2011.
531 <https://doi.org/10.3801/IAFSS.FSS.1>.
- 532 [28] H. Peel, C. Wade, M. Spearpoint, Comparison of partially lined timber room
533 experiments with the modified B-RISK flame spread capability, 14th Int. Conf. Exhib.
534 *Fire Sci. Eng. - Interflam.* (2016) 4–6.
- 535 [29] E.E. Smith, S. Satija, Release rate model for developing fires, *J. Heat Transfer.* 105
536 (1983) 281–287. <https://doi.org/10.1115/1.3245575>.
- 537 [30] T.J. Shields, G.W. Silcock, J.J. Murry, Evaluating ignition data using the flux time
538 product, *Fire Mater.* 18 (1994) 243–254. <https://doi.org/10.1002/fam.810180407>.
- 539 [31] A. Tewarson, Generation of Heat and Chemical Compounds in Fires, in: SFPE Handb.

- 540 Fire Prot. Eng., 4th ed., 2002.
- 541 [32] V. Babrauskas, Heat release rates, in: M.J. Hurley et. al (Ed.), SFPE Handb. Fire Prot.
542 Eng., 5th ed., Springer, 2016: p. 829. <https://doi.org/10.1007/978-1-4939-2565-0>.
- 543 [33] N. de Koker, R. Walls, A. Cicione, Z. Sander, S. Loffel, J. Claasen, S. Fourie, L.
544 Croukamp, D. Rush, 20 Dwelling Large-Scale Experiment of Fire Spread in Informal
545 Settlements, Fire Technol. (2020). <https://doi.org/DOI 10.1007/s10694-019-00945-2>.
- 546 [34] A. Cicione, R. Walls, Estimating time to structural collapse of informal settlement
547 dwellings based on structural fire engineering principles, in: SEMC Conf., CRC Press,
548 2019.
- 549 [35] R. Walls, G. Olivier, R. Eksteen, Informal settlement fires in South Africa : Fire
550 engineering overview and full-scale tests on “shacks ,” Fire Saf. J. 91 (2017) 997–
551 1006.
- 552 [36] M. Rosenberg, Community Based Fire Risk Reduction - Case Study of Imizamo
553 Yethu, Hout Bay, (2013).
- 554 [37] Governance Department of Cooperative Affairs South Africa., African Centre for
555 Disaster Studies, Southern Africa Society for Disaster Reduction, Per National
556 Disaster Management Centre South Africa., J. Disaster Risk Stud. 3 (2011) 443–452.
- 557 [38] E.W. Harte, I.R.W. Childs, P.A. Hastings, Imizamo Yethu: A case study of community
558 resilience to fire hazard in an informal settlement Cape Town, South Africa, Geogr.
559 Res. 47 (2009) 142–154. <https://doi.org/10.1111/j.1745-5871.2008.00561.x>.
- 560